Subhourly rainfall in a convection-permitting model

EP Meredith, U Ulbrich, HW Rust
Institut für Meteorologie, Freie Universität Berlin
edmund.meredith@met.fu-berlin.de

BINGO a better future under CLIMATE CHANGE
www.projectbingo.eu

1. Motivation and Experiment

Convection-permitting models (CPMs) have been shown to greatly improve the representation of subdaily and hourly precipitation, in particular for extreme rainfall. Intense precipitation events, however, often occur on subhourly timescales. The distribution of subhourly precipitation, extreme or otherwise, during a rain event can furthermore have important knock-on effects on hydrological processes. Little is known about how well CPMs represent precipitation at the subhourly timescale, compared to the hourly.

Here we perform multi-decadal simulations with CCLM at 0.02° resolution for a domain centred over Catalonia (Fig. 1); simulations are July - October timeslices from 1996 to 2018. We compare the CCLM output with a high-density network of precipitation gauges from the city of Barcelona at temporal resolutions of 5, 15, 30 and 60 minutes. Analysis is focused on the 3 months August - October (ASO), when the most intense precipitation in Barcelona typically falls. Boundary conditions for the CPM come from 0.11° CCLM EURO-CORDEX simulations forced by ERA-Interim reanalysis. **All presented rainfall intensities are scaled to 5-minute resolution.**

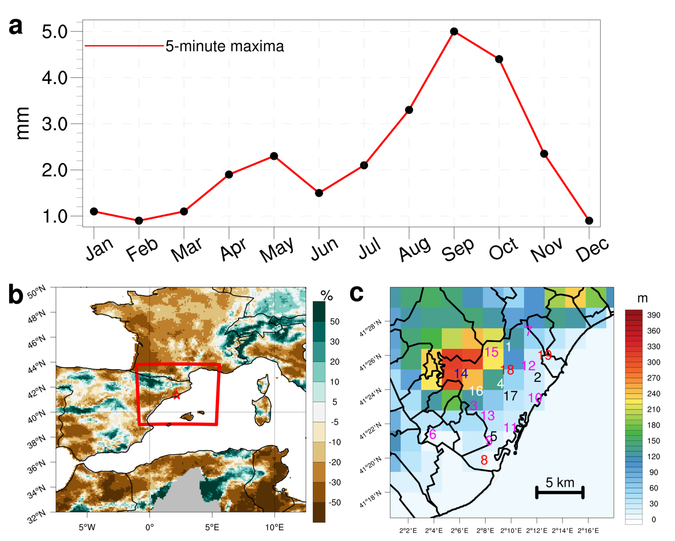


Fig. 1. Regional climatology and simulation domain.

(a) Observed annual cycle of 5 min maxima (1996-2018).

(b) CCLM-02 simulation domain (red) and ASO mean precipitation bias in parent CCLM-11 (shading)

(c) Zoom-in over Barcelona city showing CCLM-02 orography and 19 station locations.

2. Climatology and standard diagnostics

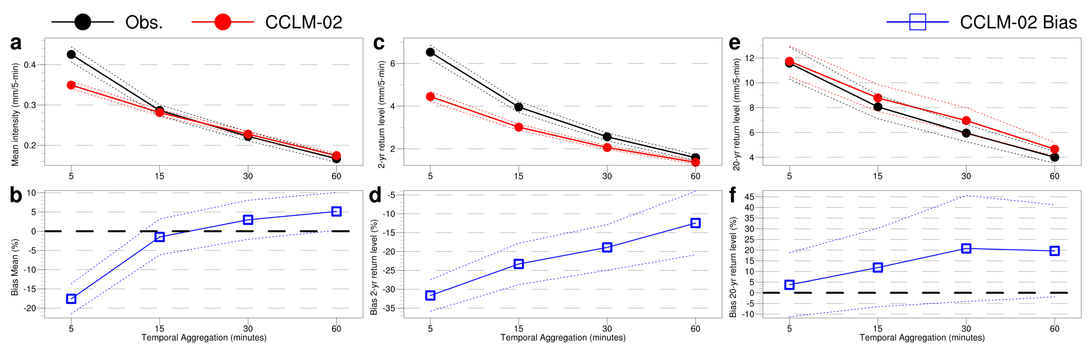


Fig. 2. Mean to extreme diagnostics as function of aggregation time. Top row shows observed and modelled diagnostics, with the CCLM-02 relative bias in the bottom row. **(a, b)** Wet-hour mean. **(c, d)** 2 year return level. **(e, f)** 20 year return level. Dashed lines show the interquartile range. Analysis for the months ASO.

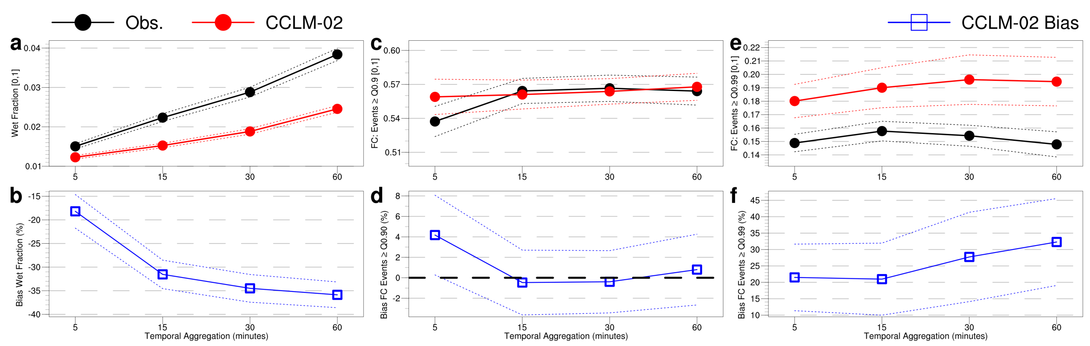


Fig. 3. Other diagnostics as function of aggregation time. (a, b) Wet-hour fraction. **(c, d)** Fractional contribution of events above the 0.9 quantile. **(e, f)** Fractional contribution of events above the 0.99 quantile. Otherwise as in Fig. 2.

3. Observed and modelled distributions

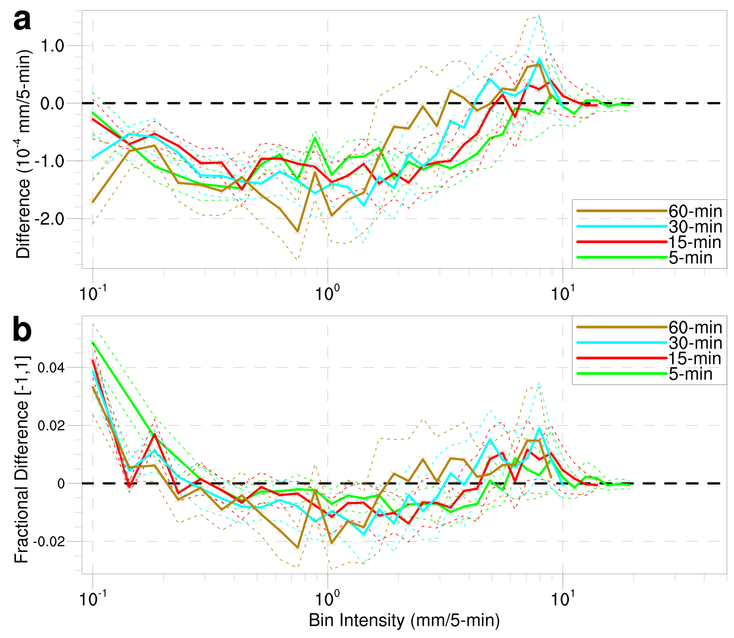
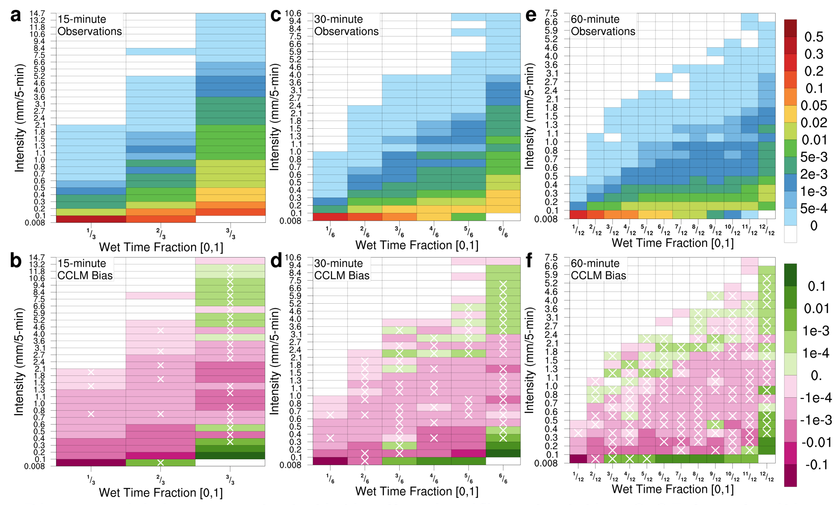


Fig. 4. Biases in (a) contribution and (b) fractional contribution to mean precipitation across precipitation spectrum.

Computations are for discrete precipitation bins based on the ASoP method proposed in Klingaman et al. (2017).

Results are shown for all aggregation times, with intensities scaled to 5-minute resolution for ease of comparison.

4. Intensities and temporal characteristics



Biases which are not statistically significant at the 0.05 level with respect to interannual variability, based on 1,000 bootstrap resamples, are struck through in white.

Fig. 5. Joint probability distribution function (JPDF) of 'wet time fraction' and event intensity.

(a, c, e) JPDFs for observations at 15, 30 and 60 min resolution.

(b, d, f) Bias of CCLM-02 with respect to observed JPDF at 15, 30 and 60 min resolution.

The *wet time fraction* is the fraction of 5 min blocks during an accumulation period in which precipitation is recorded.

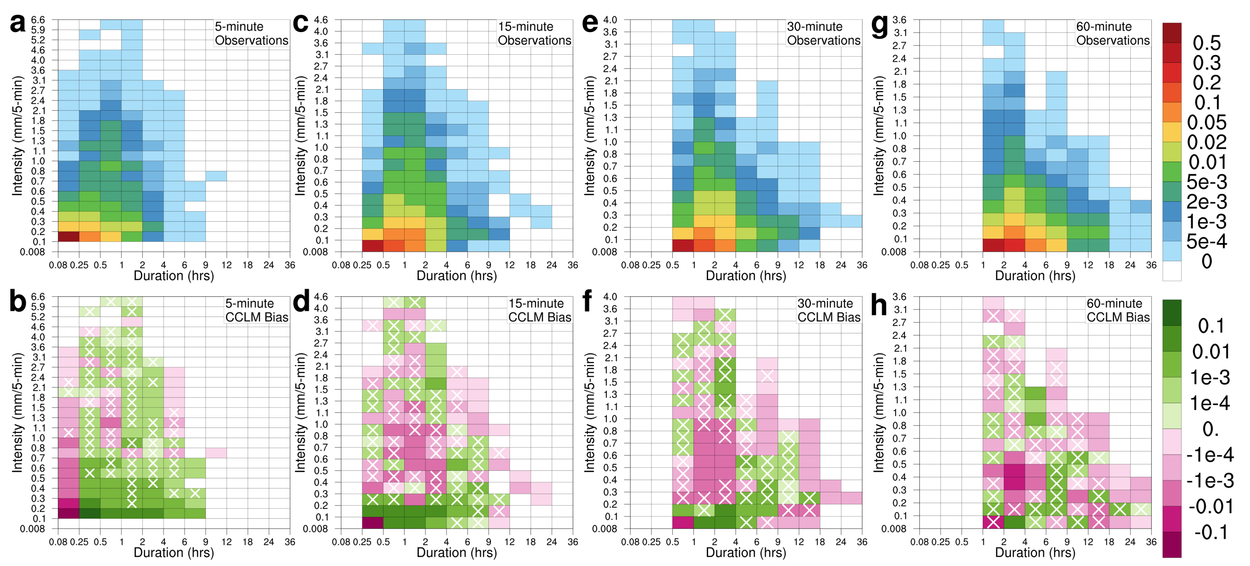


Fig. 6. JPDF of wet-spell duration and intensity.

(a, c, e, g) JPDFs for observations at 5, 15, 30 and 60 min resolution. **(b, d, f, h)** Bias of CCLM-02 with respect to observed JPDFs. Biases which are not statistically significant at the 0.05 level with respect to interannual variability, based on 1,000 bootstrap resamples, are struck through in white.

5. Spatial realism

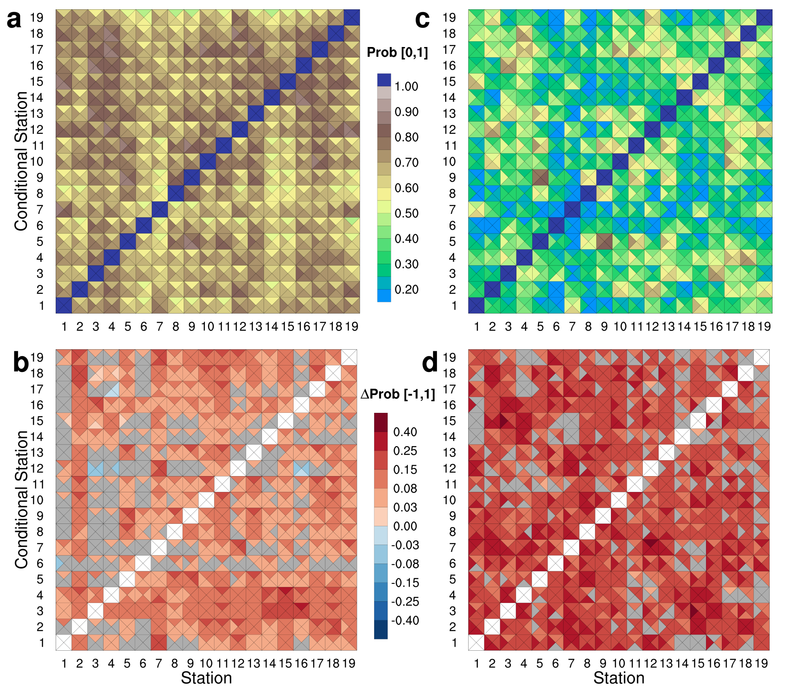


Fig. 7. Probability of a precipitation threshold being exceeded at a given station conditional on an exceedance at another station.

See figure 1(c) for station locations.

(a, c) Observed conditional probabilities for wet ($P \geq 0.1$ mm) and 0.999-quantile events.

(b, d) CCLM-02 bias for wet and 0.999-quantile events.

Biases which are not statistically significant with respect to interannual variability are shaded grey.

Each square is divided into 4 triangles which represent, clockwise from top, 5, 15, 30 and 60 min aggregations. For each station (x-axis), the probability that a given precipitation threshold is exceeded, conditional on that threshold also being exceeded at the same time at another station (y-axis), is computed.

6. Temperature scaling of precipitation

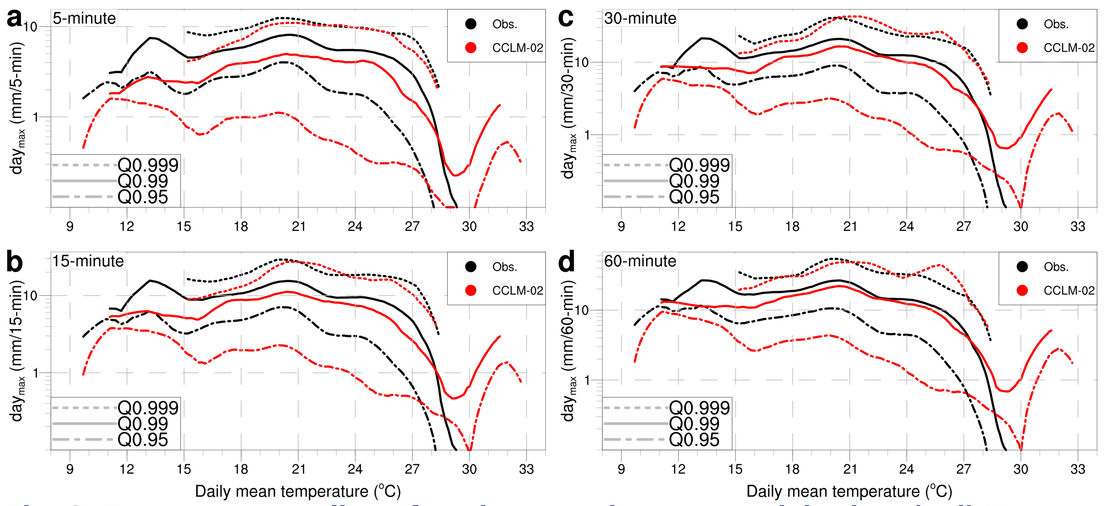


Fig. 8. Temperature scaling of moderate to intense precipitation. (a-d) Temperature scaling of the 0.95-, 0.99- and 0.999-quantiles at 5, 15, 30 and 60 min aggregations, respectively; note logarithmic y-axis.

7. Summary and Conclusions

→ **Biases at subhourly resolution no worse than at hourly resolution**

→ Insufficient contribution of moderate intensity events to mean precipitation

→ Limitations of observations relevant: strongest biases for short-duration, low-intensity events, exactly where tipping-bucket gauges have highest systematic errors. Hence large uncertainty in these biases

→ CCLM-02 excels in simulation of extremes; realistic temperature scaling

→ Results add confidence to modelling studies involving subhourly CPM precipitation, e.g. projections or hydrological modelling

→ Full study in *Env. Res. Letters* [Meredith et al., 2020]

Acknowledgements and References

The BINGO project has received funding from the European Union's Horizon 2020 Research and Innovation programme, under the Grant Agreement number 641739.

Klingaman et al. (2017): ASoP (v1.0): a set of methods for analyzing scales of precipitation in general circulation models, *Geosci. Model Dev.*, 10, 57–83.
Meredith et al. (2020): Subhourly rainfall in a convection-permitting model, Environmental Research Letters, 15(3), 034031.
ERA-Interim: Dee et al. (2011). The ERA-interim reanalysis: configuration and performance of the data assimilation system. *Q.J.R. Meteor. Soc.*, 137(656):553-597.